Available online at www.CivileJournal.org

Civil Engineering Journal

(E-ISSN: 2476-3055; ISSN: 2676-6957)

Vol. 9, No. 08, August, 2023

Mechanical and Postfire Structural Performances of Concrete under Elevated Temperatures

Vishal Murugan [1], Alireza Bahrami [2*], Rakshit Srivastava [1], K. S. Satyanarayanan [1*], Prakash Murugan [1], J. S. Arvind [3]

[1] Department of Civil Engineering, College of Engineering and Technology, SRM Institute of Science and Technology, SRM Nagar, Kattankulathur, Tamil Nadu-603203, India.

[2] Department of Building Engineering, Energy Systems and Sustainability Science, Faculty of Engineering and Sustainable Development, University of Gävle, 801 76 Gävle, Sweden.

[3] Design Group Engineering Consultant LLC, Muscat, Oman.

Received 27 March 2023; Revised 03 July 2023; Accepted 12 July 2023; Published 01 August 2023

Abstract

This article investigates the mechanical and postfire structural performances of concrete under elevated temperatures (200°C, 400°C, 600°C, and 800°C) after 7 and 28 days of concrete curing. The main objective of this study is to evaluate the post-fire behavior of concrete structures and how their modulus of elasticity values influence their structural parameters. Mechanical studies, namely, the compressive strength, splitting tensile strength, and flexural strength, were performed on cubes, cylinders, and prism beams under normal and elevated temperatures. Non-destructive tests, like rebound hammer and ultrasonic pulse velocity, were also conducted on concrete cubes to obtain the strength of concrete before and after heating the specimens. Microstructural studies, in particular, scanning electron microscope and energy dispersive x-ray spectroscopy, were done to analyze the changes in the chemical composition of concrete under the effect of the temperatures. The weight loss of the concrete specimens was assessed under the elevated temperatures. The results indicated that the geometric shapes of the specimens influenced the loss in the moisture content of concrete under an elevated temperature scenario. Microstructural studies revealed the changes in the chemical composition under the elevated temperatures. The results of this research can be further integrated for industrial applications.

Keywords: Post-Fire Structural Performance; Elevated Temperature; Geometric Shape; Mechanical Behavior; Microstructural Studies.

1. Introduction

In our overpopulated rapidly expanding world, increasing economic demand is essential for maintaining the world's population. This dense population resides in skyscrapers, which require less space and are simple to maintain while providing people with the necessities of life. The height of the building poses a number of difficulties. The design of the structure and the choice of materials for the building, which include many factors like lightweight, wind and earthquake resistance, geotechnical investigations, basement provisions, efficient vertical transportation systems, fire safety, speed of construction, repair, maintenance, efficient plumbing systems, and usage of information technology, are the main challenges of tall buildings. A high-rise building makes sense as a successful building for the people's use when all the fundamental prerequisites are satisfied. In the unlikely event that an important failure happens, it is equally crucial to save the lives of the inmates. A common failure that must be prevented is the one that is catastrophic and typically progresses over time.

* Corresponding authors: alireza.bahrami@hig.se; satyanak@srmist.edu.in

http://dx.doi.org/10.28991/CEJ-2023-09-08-04

© 2023 by the authors. Licensee C.E.J, Tehran, Iran. This article is an open access article distributed under the terms and conditions of the Creative Commons Attribution (CC-BY) license (http://creativecommons.org/licenses/by/4.0/).

Concrete is one of the major construction materials employed in the construction industry. Concrete is made up of a mixture of cement, fine aggregate, coarse aggregate, and water to obtain the desired strength. Concrete has high durability and serviceability, which favors its massive usage in the construction industry. There are several factors that affect the durability and serviceability of concrete, and one such concern is fire [1, 2]. Whenever a concrete structure is subjected to fire accidents, concrete undergoes the effects of high temperatures. Concrete undergoes both physical and chemical changes when it is subjected to high temperatures [2, 3]. The concrete structures' ability to carry loads decreases as a result of exposure to fire conditions.

Hardened concrete consists of moisture and porous voids filled with air [4]. These voids and moisture content play a vital role in the strength reduction during fire scenarios. Over the years, researchers have toiled with boundless concrete materials at high temperatures [5]. The research works governing the basic material properties and characteristics of concrete concerning the temperature effect were found to be abundant [6]. The chemical composition changes under elevated temperatures, leading to a reduction in the strength parameters. The release of thermal stresses results in the formation of cracks on the concrete surface. The thermal effect reduces the moisture content of concrete.

Furthermore, due to the low water-cement ratio in reinforced concrete, concrete spalling under fire conditions is a major problem. Concrete spalling owing to the temperature action has been documented in real-world and laboratory situations. Spalling causes rapid concrete loss during a fire. Fire temperatures reach deeper layers of concrete. Spalling in concrete is induced by the load and heat stress.

Few researchers have worked on the in-depth characteristics of concrete at high temperatures. To ascertain how concrete's Mode 1 fracture energy depends on temperature and the precise water content, Bažant & Prat [7] performed fracture experiments on concrete at temperatures ranging from 20°C to 200°C. The reaction of concrete under combined thermal and mechanical actions was characterized by Thelandersson [8], who rejected the widely held belief that both thermal and mechanical stresses may function as independent accompanying elements. Schneider [9] used numerous tests to determine the properties of concrete to report a thorough study on the effects of high temperatures on concrete. Chan et al. [10] conducted a comparative study between high-strength concrete and normal-strength concrete under high temperatures and found the critical temperature range of concrete under high temperatures. Short et al. [11] observed color changes in concrete under elevated temperatures using optical microscopy. They concluded that their results coincided between the compressive strength and visual inspection.

For concrete subjected to cyclic loads, Lee & Fenves [12] created a plastic analysis model based on the fracture energy and stiffness degradation theory. When concrete comes into contact with fire, its properties are altered. Concrete becomes brittle when the temperature rises because the strength components decrease. A summary of the effects of high temperatures on concrete materials and structures was provided by Schrefler et al. [13]. Xu et al. [14] evaluated the role of metakaolin in a concrete mixture containing textile-reinforced concrete at high temperatures. They found the bond characteristics of textile-reinforced concrete through the microstructural analysis. Varghese et al. [15] assessed the influence of fibers in concrete under elevated temperatures. They found that carbon fibers enhanced the bond strength of concrete at high temperatures.

Zhao et al. [16] carried out the microstructural analysis and strength determination tests on polymer concrete under dry environmental conditions. The microstructural analysis depicts the hydration process in concrete due to dry heat conditions. Abolhasani et al. [17] investigated the fracture features, microstructural properties, and mechanical characteristics of calcium aluminate cement concrete. They found that the residual fracture toughness and the strength parameters deflated as the temperature increased. Phan & Carino [18] conducted a valuable compendium of experimental data on the mechanical characteristics of high-strength concrete under elevated temperatures. Handoo et al. [19] studied the physical and chemical properties and characteristics of concrete at high temperatures through scanning electron microscopy. Figure 1 shows the temperature-related physical changes in concrete due to fire [3].

Nechnech et al. [20] evaluated transient creep models of concrete using the thermomechanical analysis. Shin et al. [21] observed the erosion rate and thermophysical properties of concrete under elevated temperatures of up to 1100℃. Willam et al. [22] discovered damage to bonding characteristics in concrete material under mechanical and thermal loading conditions. Youssef & Moftah [23] proposed a relationship for stress-strain and other parameters, such as the transient creep, bond strength, and yield properties of steel and concrete under high temperatures. Caetano et al. [24] did an experimental investigation to witness the fractural energy at normal and high temperatures of high-strength polypropylene and steel fiber concrete. They found disintegration of the fractural energy and ultimate strength characteristics with respect to temperature. Reddy & Ramaswamy [25] evaluated the high-temperature effect on various concretes under the influence of different admixtures and aggregates. The observations from the studies demonstrated that the residual strength of concrete varied under high-temperature conditions.

Concrete exposed to heat exhibits a variety of behaviors, including changes in the strength, durability, and serviceability. The post-fire condition is often very critical, as concrete has already lost its stiffness due to fire. Understanding these parameters and how they affect the nature of reinforced concrete structures gives better clarity on the thermal effects that concrete undergoes. Hence, a detailed study is carried out to find the effect of fire on the internal and external characteristics of concrete and their post-fire behavior. The main purpose of this study is to achieve the influence of geometric shapes on the weight loss under fire conditions and post-fire structural performance under reduced modulus of elasticity values due to fire.

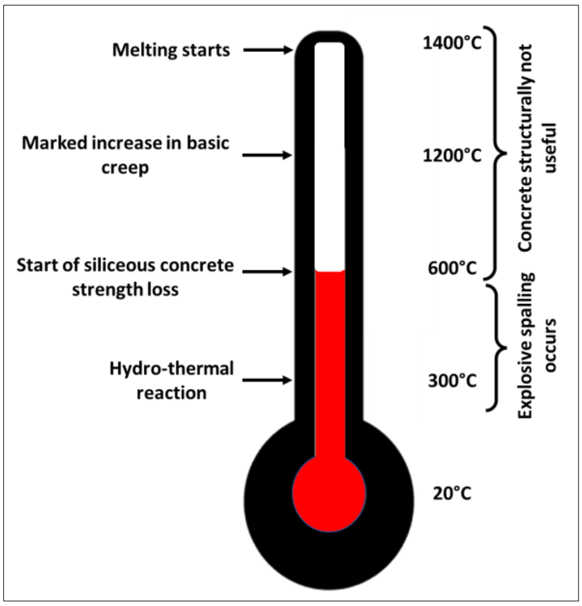

Figure 1. Physical changes in concrete under fire [3]

The mechanical and post-fire structural performances of concrete under elevated temperatures (200°C, 400°C, 600°C, and 800°C) after 7 and 28 days of concrete curing are presented in this article. A post-fire condition is determined from the observed modulus of elasticity of concrete under the elevated temperatures, and a real structural model is analyzed using STAAD Pro v8i.

2. Materials and Methodology

M30-grade concrete was prepared with a mix ratio of 1:1.77:1.9 and a water-cement ratio of 0.45. The mix ratio was designed as per the standard [26]. Ordinary Portland cement (OPC) of grade 53 was utilized along with river sand and 10 mm coarse aggregates. The grading curves for the used river sand and cement are illustrated in Figure 2. The specific gravities of the materials are listed in Table 1.

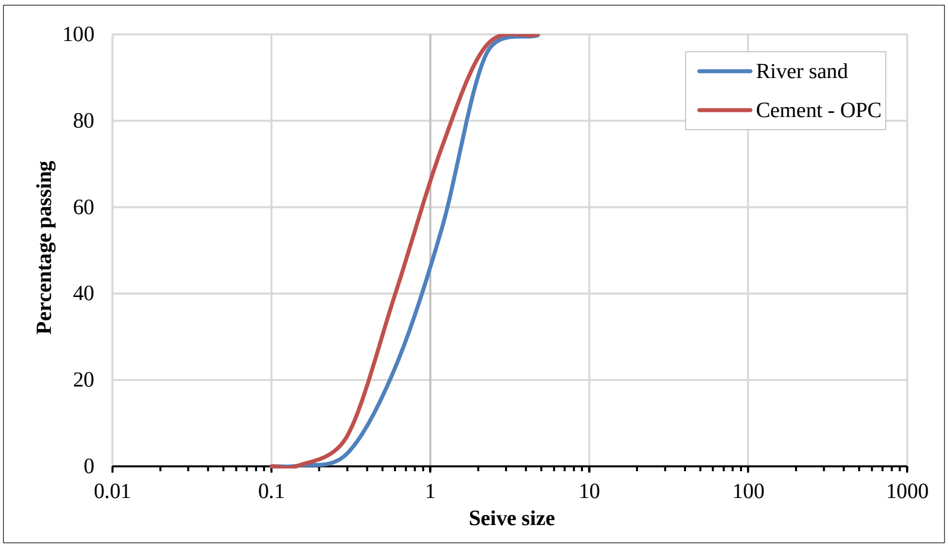

Figure 2. Grading curves for materials

Table 1. Specific gravity values of materials

Description	Specific gravity
Cement	3.15
Fine aggregate (river sand)	2.60
Coarse aggregate	2.81

Cubes, cylinders, and flexural beams were utilized in this study to determine the effect of the elevated temperatures on compressive, splitting tensile, and flexural performances. The specimens were tested at the room temperature (assumed to be 29°C), 200°C, 400°C, 600°C, and 800°C. The dimensions of the cubes, cylinders, and flexural beams are given in Table 2.

Table 2. Dimensions of cubes, cylinder, and flexural beams

Description	Dimension (mm)
Cube (length × breadth × height)	100 × 100 × 100
Cylinder (diameter × height)	100 × 200
Flexural beam (length × breadth × height)	500 × 100 × 100

To perform the tests, three specimens were employed for each temperature condition, and the results were taken from the average of the three specimens. Water curing was done until the 7th and 28th days after casting the specimens. The specimens were temperature treated after the 7th and 28th days, and several tests were conducted. For heating the concrete specimens, a heating furnace with a capacity of 1200°C was used. All the specimens were weighted before and after the temperature treatment. Similarly, initial readings were taken for non-destructive testing. Care was taken while removing the specimens from the heating furnace. After the specimens were naturally air-cooled, all the specimens were weighted and tested. Figure 3 displays the concrete specimens placed inside the heating furnace before testing.

Figure 3. Specimens placed inside heating furnace

After heating the specimens, tests were performed to determine the mechanical properties of concrete, and a post-fire analysis was done. The entire flow of the research work is depicted in Figure 4.

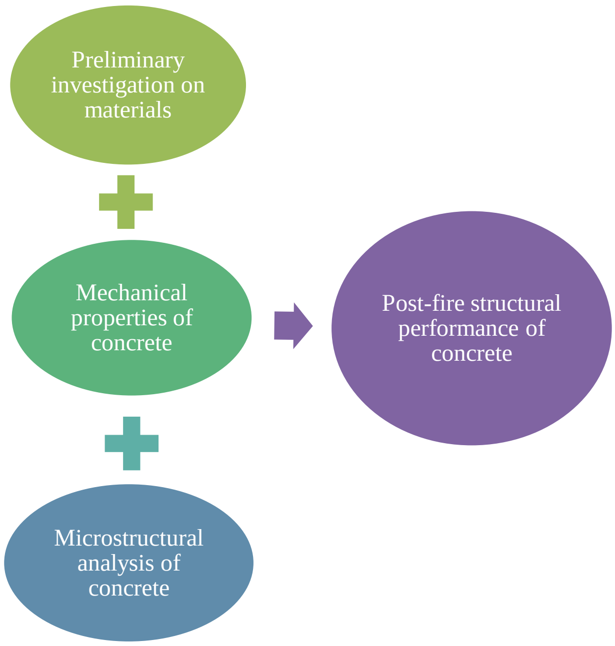

Figure 4. Flow of research work

3. Results and Discussion

3.1. Preliminary Investigation

3.1.1. Surface Cracks

After heating the specimens, a visual inspection was conducted, and the color change and intensity of cracks due to the heat were noted. The surface cracks were observed after the temperature treatment and are demonstrated in Figure 5. The change in color was seen in the specimens at the temperatures of 600°C and 800°C. Similarly, visible cracks were also witnessed in the specimens at 600°C and 800°C. At 400°C, no visible cracks were formed on the surface. The cracks might have developed internally, but they did not propagate toward the external surface. In all the cases, the cracks that developed at 7 days were larger than those at 28 days. This indicated the importance of proper curing in the case of fire scenario. Surface cracks influenced the durability of concrete as they created a path for acidic moisture to ingress, which eventually corroded the rebars inside.

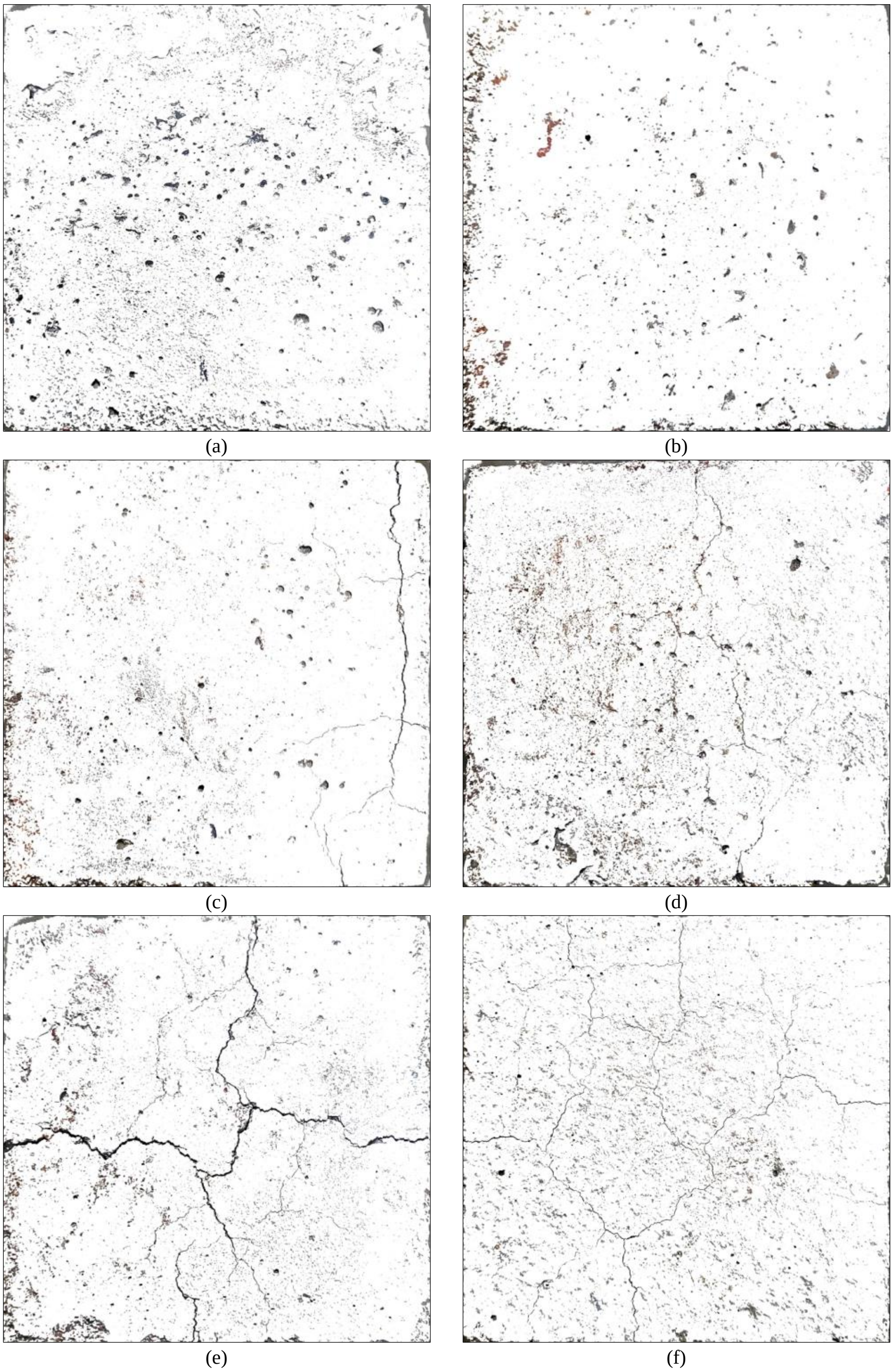

Figure 5. Surface crack patterns in cube specimens (a) 400°C at 7 days (b) 400°C at 28 days (c) 600°C at 7 days (d) 600°C at 28 days (e) 800°C at 7 days (f) 800°C at 28 days

3.1.2. Weight Loss in Concrete under Temperature

Curing of concrete plays an essential role in enhancing its strength. Curing of concrete aids in the formation of gel, which directly influences the strength. Concrete releases heat during the process of hydration. This heat significantly leads to plastic shrinkage cracks, which result in the degradation of the strength. After demolding, the water curing process must be initiated for the minimum curing duration of 7 days. The absorbed moisture content was reduced during the heating process. The reduction in moisture increased with respect to the temperature. The reduction in moisture content influenced the strength reduction factor under the temperature effect. The comparisons of the percentages of average weight losses in the cubes, cylinders, and flexural beams observed after 7 and 28 days of curing and after heating are shown in Figures 6 to 8.

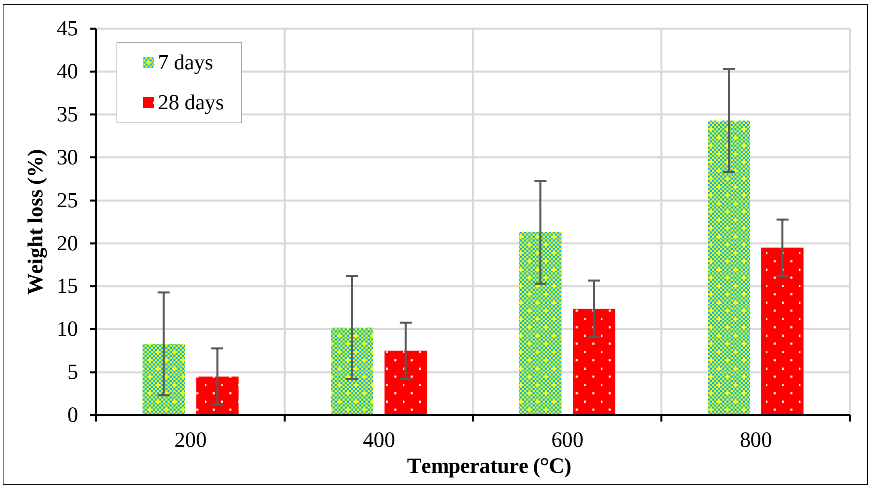

Figure 6. Percentage of weight loss in cubes after heating

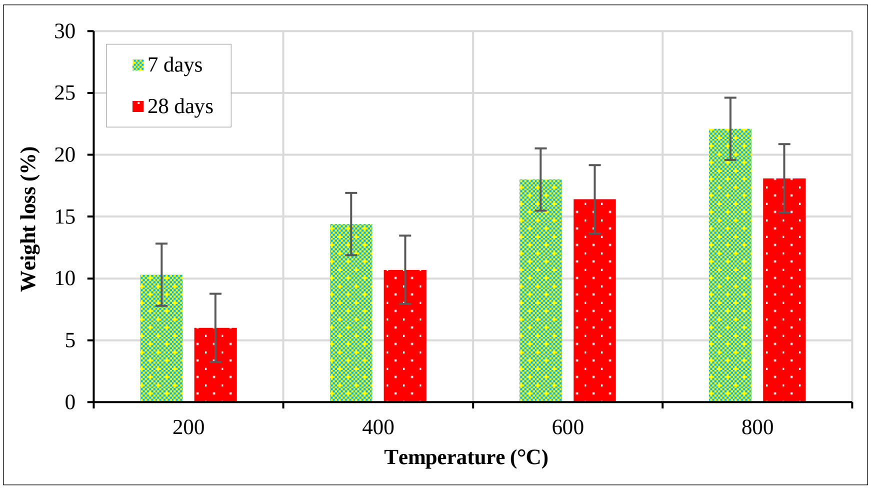

Figure 7. Percentage of weight loss in cylinders after heating

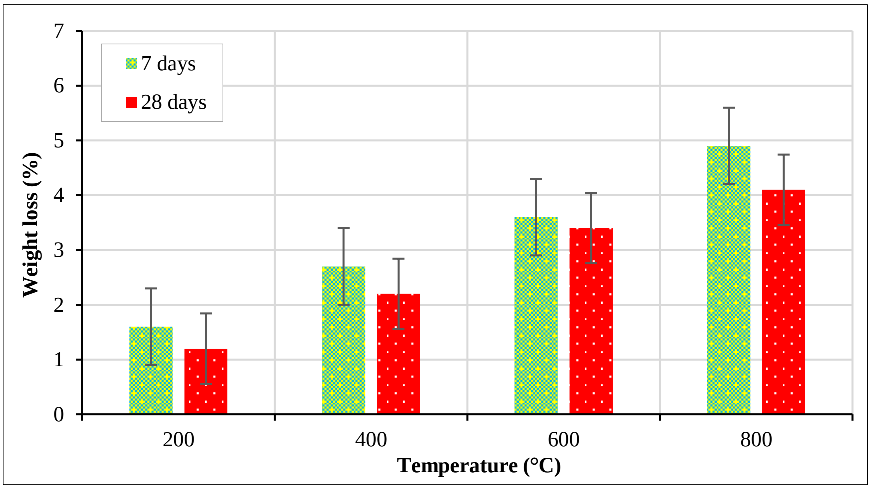

Figure 8. Percentage of weight loss in flexural beams after heating

Cubes underwent a massive reduction in weight after heating compared to cylinders and flexural beams. This issue revealed the effect of volume on the weight reduction after heating. At 800°C, the cubes had reductions of approximately 34.3% and 19.5% for 7 and 28 days, respectively. Similarly, for cylinders, they were 22.1% and 18.1%, and for flexural beams, they were 4.9% and 4.1%.

3.1.3. Non-Destructive Testing

Non-destructive testing is usually carried out to assess the quality of materials or specimens without damaging them. The rebound hammer and ultrasonic pulse velocity tests are the two non-destructive tests conducted in this study before and after heating the specimens. The rebound hammer test was performed to determine the surface hardness of the concrete specimens. The rebound hammer has a tip that is pressed against the concrete surface, and the corresponding value is displayed. The value denotes the surface hardness or elastic nature of the concrete specimens. The tests were conducted on concrete cubes before and after the temperature treatment, and the average numbers were taken. Figure 9 illustrates the rebound number for concrete cube specimens before and after the temperature treatment. The rebound number was witnessed for the specimens at the room temperature, 200°C, and 400°C, however, the specimens at 600°C and 800°C on the 7th day completely cracked due to the temperature effect, therefore, their values were not displayed. The reduction in the rebound number indicated the loss in the elastic nature of concrete under the elevated temperatures.

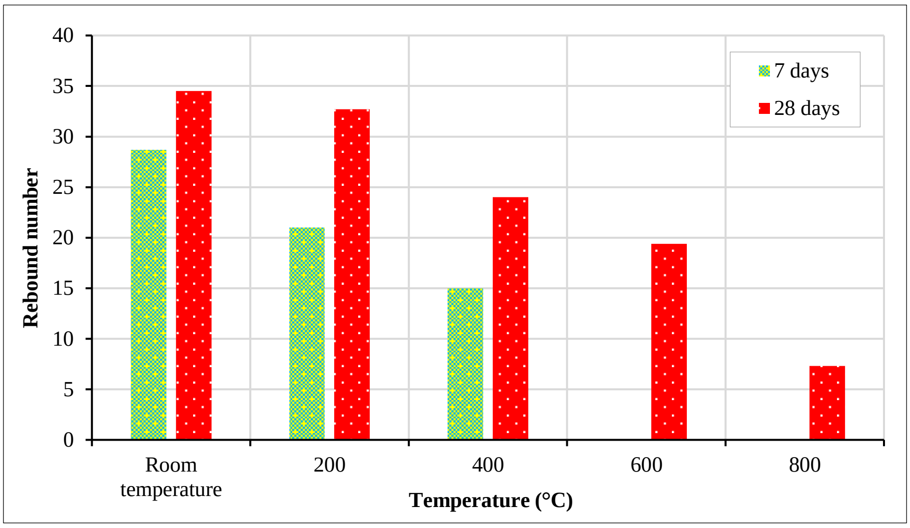

Figure 9. Rebound number for concrete cubes at room temperature and temperature-treated specimens

The ultrasonic pulse velocity test was done by calculating the time taken for the pulse to travel across the concrete cubes. This test was performed to determine the internal cracks on the tested specimens and air voids in the hardened concrete. The pulse waves were generated by the transmitter and acquired by the receiver at the other end. A direct approach was employed in this study. The distance travelled by the pulse and the time taken gave the velocity. Figure 10 presents the velocity for the concrete cube specimens before and after the temperature treatment.

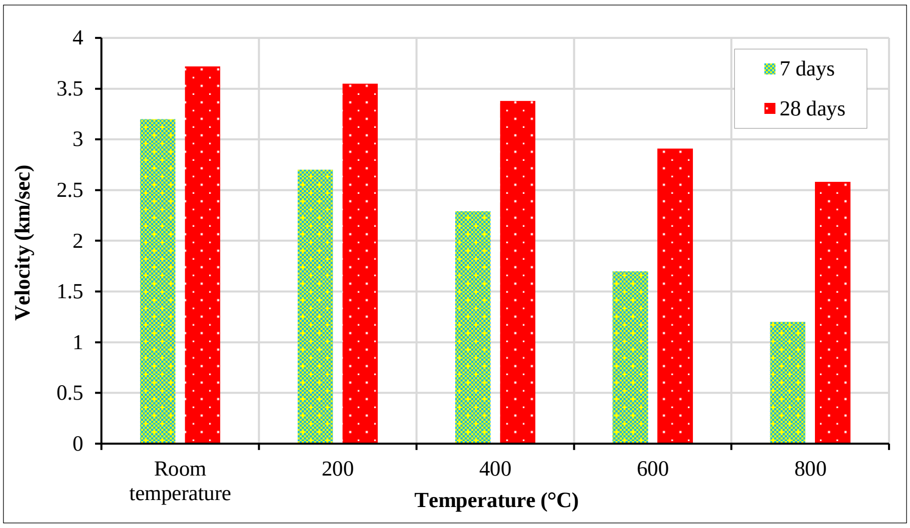

Figure 10. Velocity of concrete specimens at various temperatures

The time taken for the waves to transmit increases if the specimen has more air voids or cracks. Cracks are induced in concrete as it is subjected to high temperatures. This significantly increases the transmission time of the waves. As a result, the velocity gradually decreased with respect to the elevated temperatures. The drop was gradual until 400°C, after which the drop was slightly higher at 600°C. This demonstrated the failure of the specimens as a result of widening of cracks due to the temperature increase.

3.2. Strength Parameters

3.2.1. Compression Test on Cubes

The compression test was conducted on the cubes to obtain the compressive strength of concrete. The compression test was done on the cube specimens after 7 and 28 days of curing. The test was performed on three specimens for each temperature, and the average values were taken. The average compressive strengths of the cubes under the elevated temperatures are presented in Figure 11.

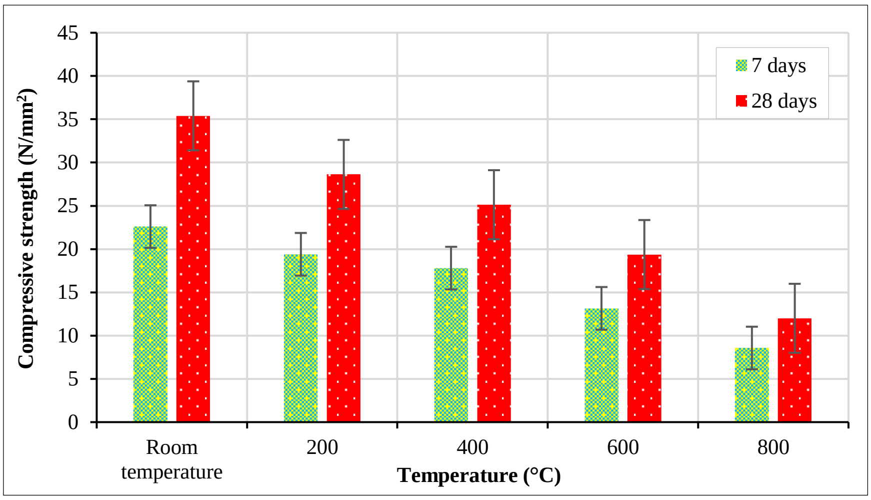

Figure 11. Average compressive strengths of cubes at various temperatures

As per [27], the design strength of concrete should attain 70% of its target mean strength after 7 days of curing. The results clearly indicated that the initial compressive strength was attained after 7 days of water curing. The strength gradually decreased with the temperature increase [28]. There was a sudden drop after 400°C, which revealed a reduction in the compressive characteristics of concrete after 400°C at a large scale, as was also reported in the previous studies [29].

3.2.2. Splitting Tensile Test on Cylinders

The splitting tensile test was used to identify the tensile nature of concrete. The splitting tensile test was conducted on the cylinder specimens after 7 and 28 days of curing. The same numbers of the specimens were tested as in the above-mentioned case. The average splitting tensile strengths of the cylinders at several temperatures are represented in Figure 12. The splitting tensile strengths of the concrete cylinders degraded with respect to the temperature increase, like the previous case. The drop after 400°C denoted a greater loss in the tensile nature of concrete.

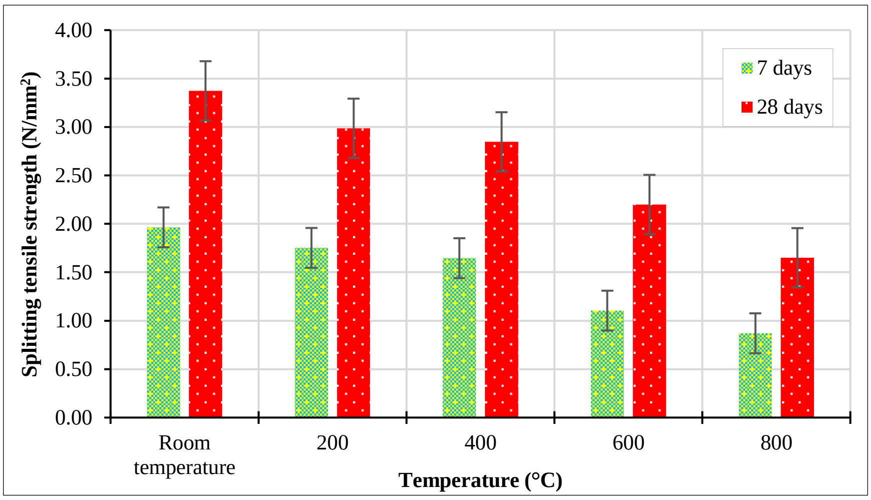

Figure 12. Average splitting tensile strengths of concrete cylinders at various temperatures

At the room temperature, the splitting tensile strength of concrete on the 28th day was 1.7 times higher than that of the 7th day. But in the case of 800°C, it was 1.9. This elaborated on the impact of extreme temperature conditions, as there was no internal bond in the concrete matrix.

3.2.3. Flexural Test on Flexural Beams

The flexural test was performed to obtain the flexural strength of concrete. The flexural test was done by applying pure bending alone. The flexural test was conducted on the flexural beams after 7 and 28 days of curing, similar to the previous cases. The average flexural strengths of the flexural beams at several temperatures are depicted in Figure 13. The results of the flexural strength tests resembled the previous cases. The strengths deflated with respect to the temperature increase, and the drop in the flexural strength was greater after 400°C. This reduction implied the decline in the flexural capacity of concrete owing to the temperature increase.

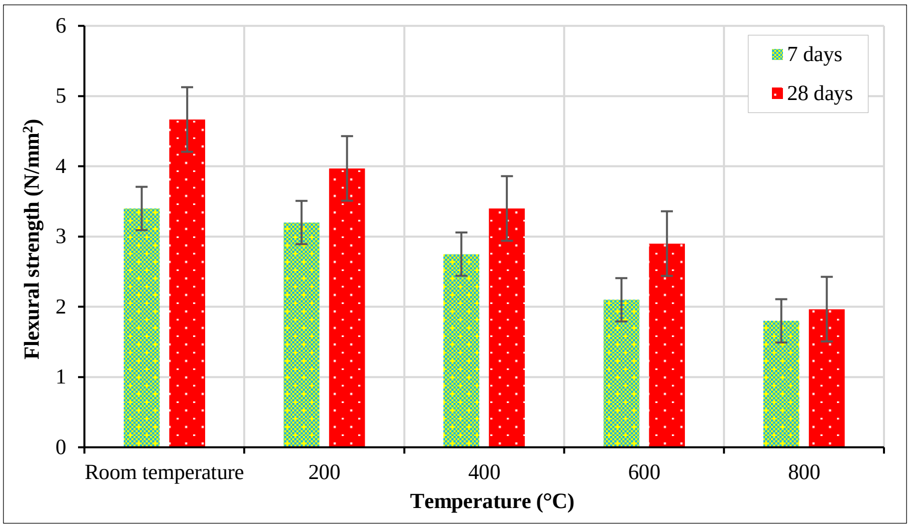

Figure 13. Average flexural strengths of flexural beams at various temperatures

At the room temperature, the flexural strength of concrete on the 28th day was 37% higher than that of the 7th day. But in the case of 800°C, it was 9.4%. The flexural strength reduced drastically at the extreme temperatures, which could increase the deflections in concrete beams.

3.3. Internal Behavior

3.3.1. Microstructural Analysis

The scanning electron microscope (SEM) images of the interface between the cement matrix and concrete reaction were analyzed at different curing ages and temperatures (200–800°C) [30, 31]. At 200°C, the SEM view of the concrete specimens revealed the shrinkage of the cement paste, the formation of microcracks brought on by the chemical and physical losses of water, and ettringite breakdown. On the other hand, the cement paste became denser than before as a result of the increased rate of hydration that created extra hydration due to the temperature variation, particularly calcium aluminate hydrates (CAH) and calcium silicate hydrates (CSH) gel formation, as shown by SEM images from specimens of all mixes with nanoparticles. This might be a result of the slow heat transfer of the nanoparticles compared to the heat transfer of conventional concrete because of their low thermal conductivity. Figure 14 displays the SEM images and energy dispersive x-ray spectroscopy (EDS) analysis results of the impact of the temperature (200°C) on concrete.

Compared to concrete at the room temperature, there was a slight difference in the heat of the hydration action, and there was not much difference in the chemical characteristics of concrete at different ages. Cement plays a major role in the CSH gel formation in the transition zone to improve the durability of concrete at later ages. The compressive strength of concrete reached a maximum value of 30 N/mm², which was nearest to the conventional concrete specimen at the room temperature. Compared to 200°C, at 400°C, the concrete voids increased and gradually increased the density of the ash formation. At 13000X magnification in SEM, concrete became brittle due to the heat absorption. Figures 15a and 15c illustrate the crack propagation in concrete.

While comparing Figures 14 and 15, the internal phase of concrete was examined at 5 µm. Larger amounts of ash and pore formations appeared on the 7th and 28th days of concrete, which indicated that concrete became brittle in its mechanism with the compressive strengths of 8.57 N/mm² and 12 N/mm², respectively. However, the composition of concrete molecules reduced the capillary porosity, which accelerated the formation of cement. On the 28th day of concrete at 800°C, it was pollutant concrete with un-hydrated cement grains, and its result decreased by approximately 20–30% of its standard compressive strength. The microstructural analysis was done using the SEM images and EDS analysis, and different temperatures were studied on M30-grade concrete at different ages of 7 and 28 days. The magnification of the SEM imaging revealed the detailed phase of concrete in a 5 µm view, and EDS was compared with the performance analysis of the concrete specimens. With the combination of algorithms, a decrease in the compressive strength caused a temperature impact on concrete.

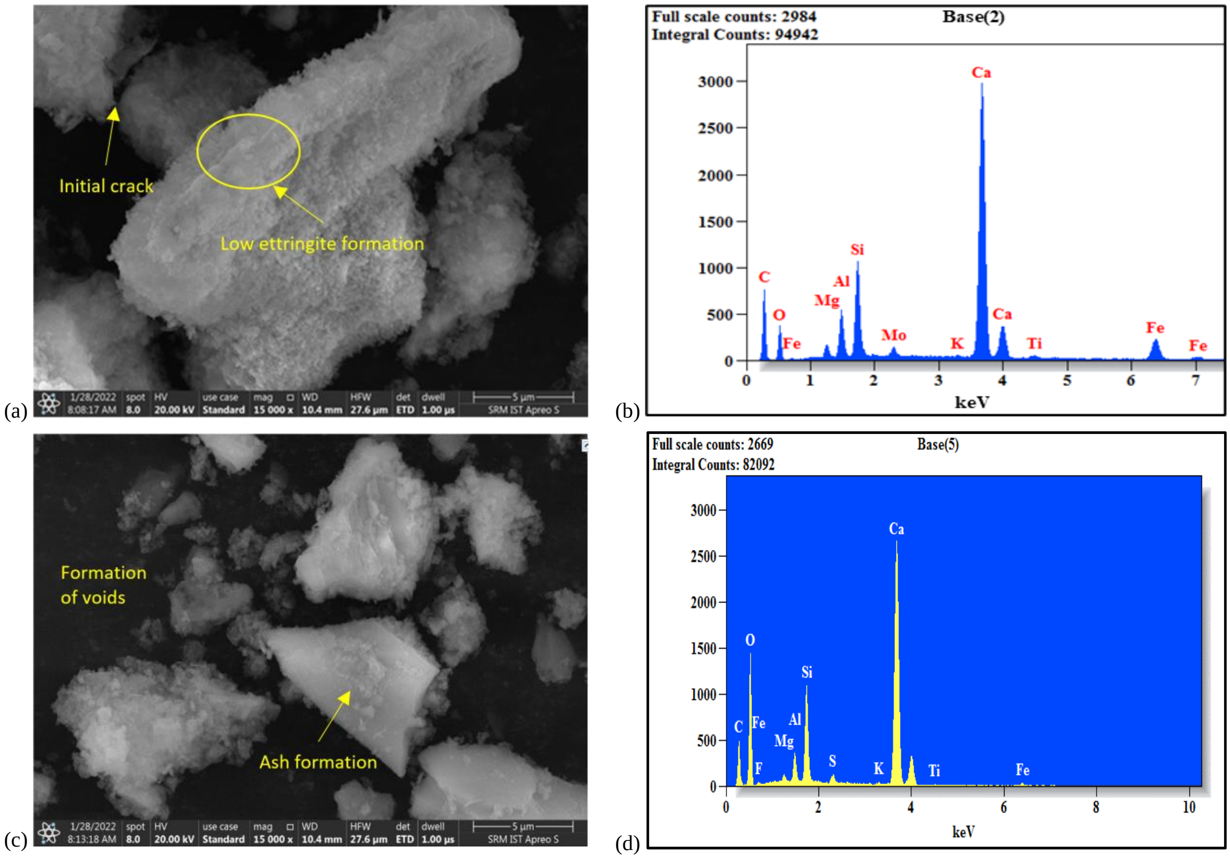

Figure 14. (a) 5 µm SEM image of M30-grade concrete at 7th day under 200℃ (b) EDS analysis of M30-grade concrete at 7th day under 200℃ (c) 5 µm SEM image of M30-grade concrete at 28th day under 200℃ (d) EDS analysis of M30-grade concrete at 28th day under 200℃

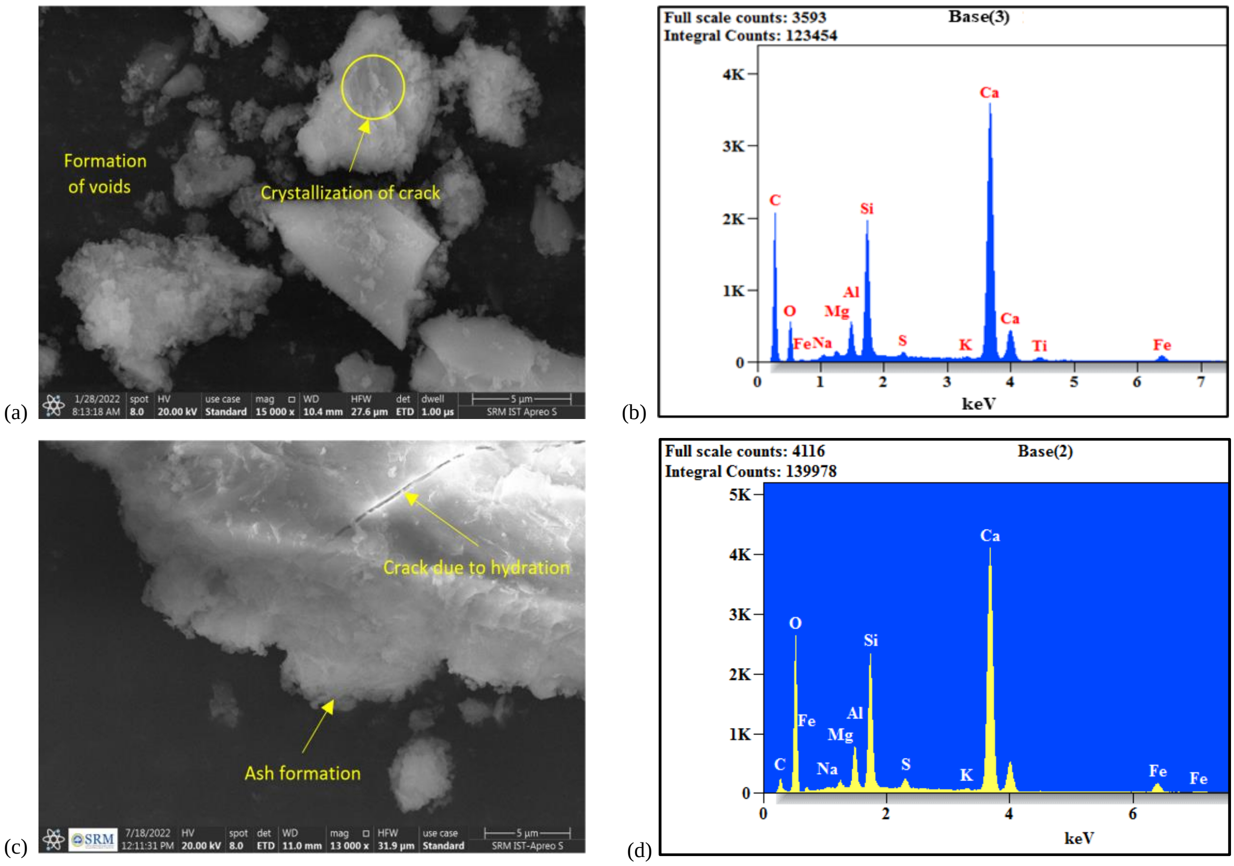

Figure 15. (a) 5 µm SEM image of M30-grade concrete at 7th day under 400℃ (b) EDS analysis of M30-grade concrete at 7th day under 400℃ (c) 5 µm SEM image of M30-grade concrete at 28th day under 400℃ (d) EDS analysis of M30-grade concrete at 28th day under 400℃

The chemical composition of concrete on the 7th and 28th days changed their own characteristics, as demonstrated in Figures 16a and 16c; the titanium action decreased on the 28th day, which caused pores to develop in concrete with maximum heat of the hydration action in the concrete observation period.

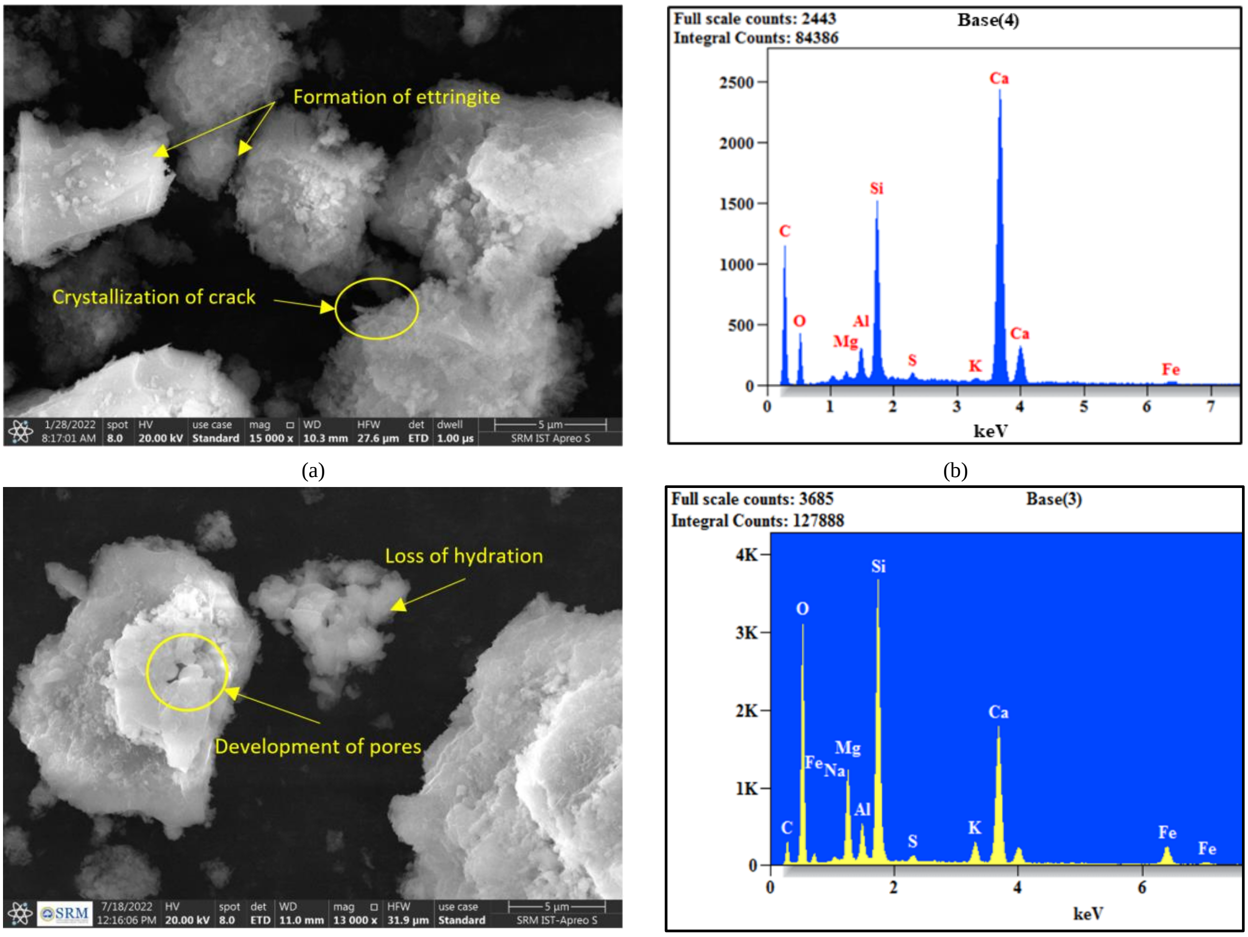

(a) (b) (c) (d)

Figure 16. (a) 5 µm SEM image of M30-grade concrete at 7th day under 600°C (b) EDS analysis of M30-grade concrete at 7th day under 600°C (c) 5 µm SEM image of M30-grade concrete at 28th day under 600°C (d) EDS analysis of M30-grade concrete at 28th day under 600°C

Additionally, pores and a significant rise in microcracks were seen. In the nanoparticle mix specimens, there was more CAH owing to the hydration process, and its concentration rose as the fraction of nanoparticles increased. At 400°C, the specimen experienced the increased breakdown of CSH and total decomposition of calcium hydrates (CH), as well as the enlargement of microcracks and holes. Microcracks started to form in the specimens; however, neither pores nor cracks appeared in the 600 °C specimens, as shown in Figure 17. Due to the loss of CSH in the specimens, their structure cracked severely, lost bonding, and fragmented at approximately 800°C. The specimens exhibit cracks and porosity up to 800°C.

3.4. Structural Behavior and Post-Fire Performance

3.4.1. Modulus of Elasticity of Specimens

The values of the modulus of elasticity of the specimens were achieved using a compressometer. The test was done at the room temperature, 200°C, 400°C, 600°C, and 800°C after 7 and 28 days of curing. The calculated values of the modulus of elasticity of the specimens are presented in Figure 18.

The modulus of elasticity values signified a drastic change after 400°C. This proved the reduction in the strength after 400°C. From the obtained modulus of elasticity values, a two-bay single-story reinforced concrete frame was validated to check the effect of the reduced modulus of elasticity values and temperature conditions. The modulus of elasticity values were analyzed in STAAD Pro V8i. Two cases were considered, namely, Case (i) with the modulus of elasticity values at the room temperature, 200°C, 400°C, 600°C, and 800°C at 28 days and Case (ii) with the reduced modulus of elasticity values (at the room temperature, 200°C, 400°C, 600°C, and 800°C at 28 days) along with the temperature effect. Table 3 lists the cases considered for the validation of the modulus of elasticity value.

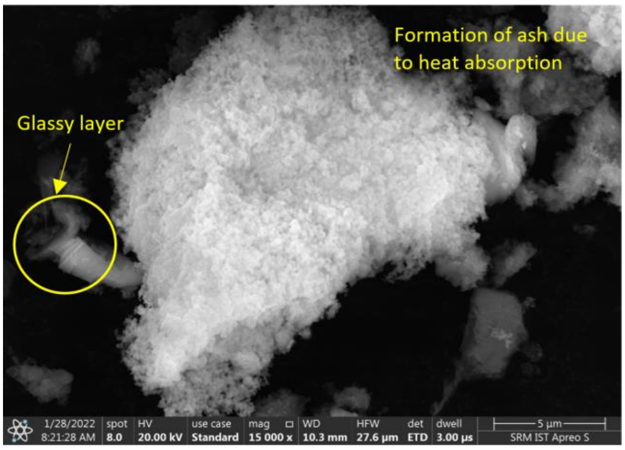

(a)

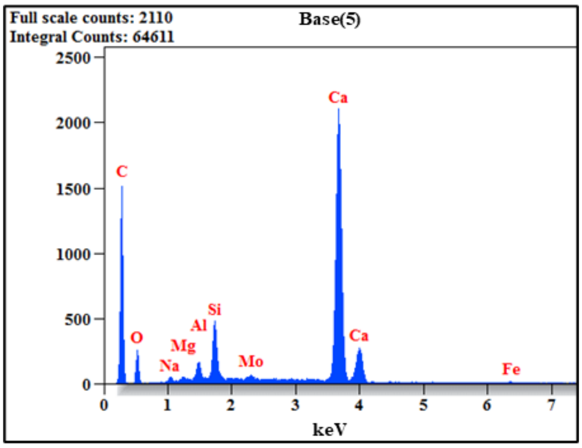

(b)

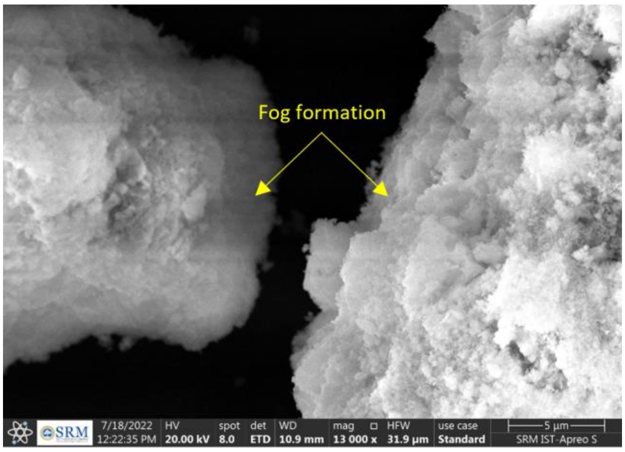

(c)

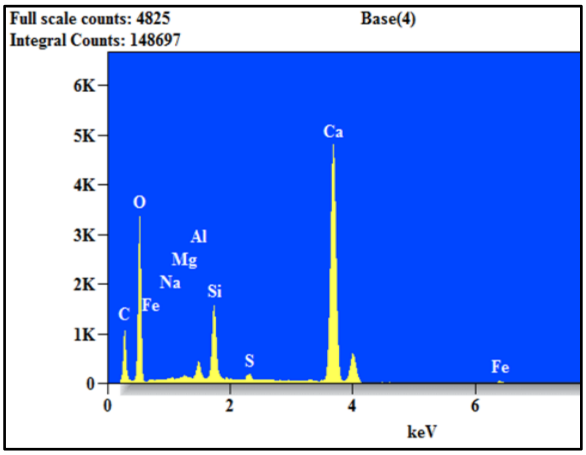

(d)

Figure 17. (a) 5 µm SEM image of M30-grade concrete at 7th day under 800°C (b) EDS analysis of M30-grade concrete at 7th day under 800°C (c) 5 µm SEM image of M30-grade concrete at 28th day under 800°C (d) EDS analysis of M30-grade concrete at 28th day under 800°C

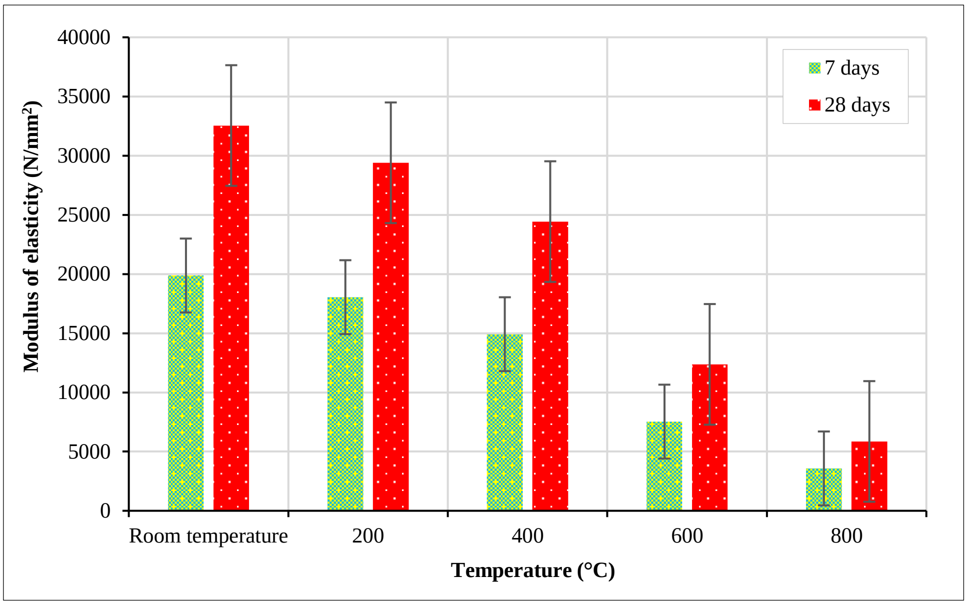

Figure 18. Modulus of elasticity values of specimens at various temperatures

The dimensions of the frame are given in Figure 19. The columns and beams had the same cross-sectional dimensions of 350 × 500 mm. The beams were provided with prestressing tendons, and the layout is depicted in Figure 20.

Table 3. Cases considered for validation of obtained modulus of elasticity (E) values

Specimen name	Case (i) E (N/mm^2)	Case (ii) E (N/mm^2) + Temperature (°C)
Room temperature	32548	32548 + room temperature
200°C	29401	29401 + 200°C
400°C	24431	24431 + 400°C
600°C	12368	12368 + 600°C
800°C	5859	5859 + 800°C

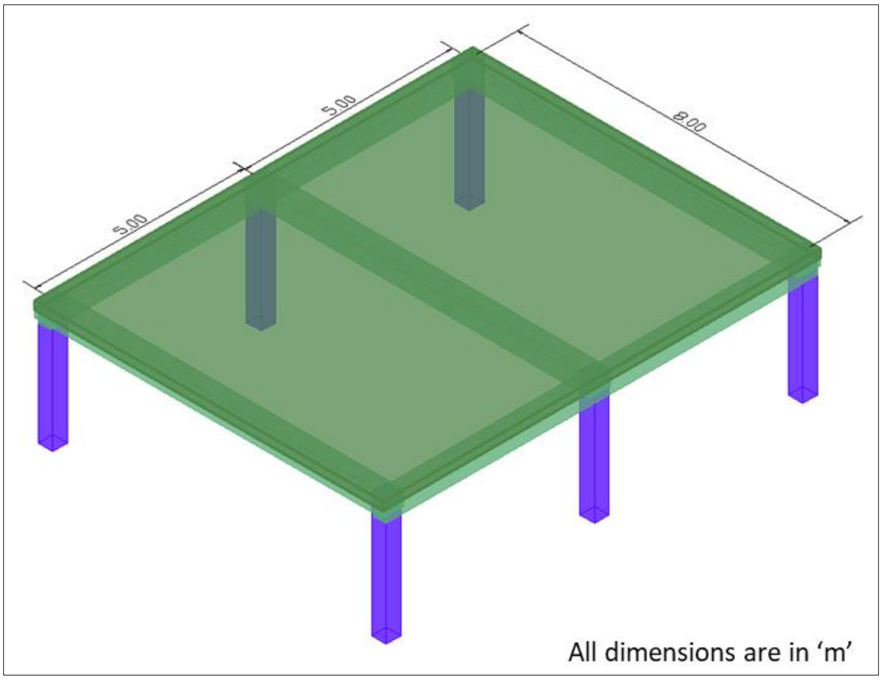

Figure 19. Dimensions of frame

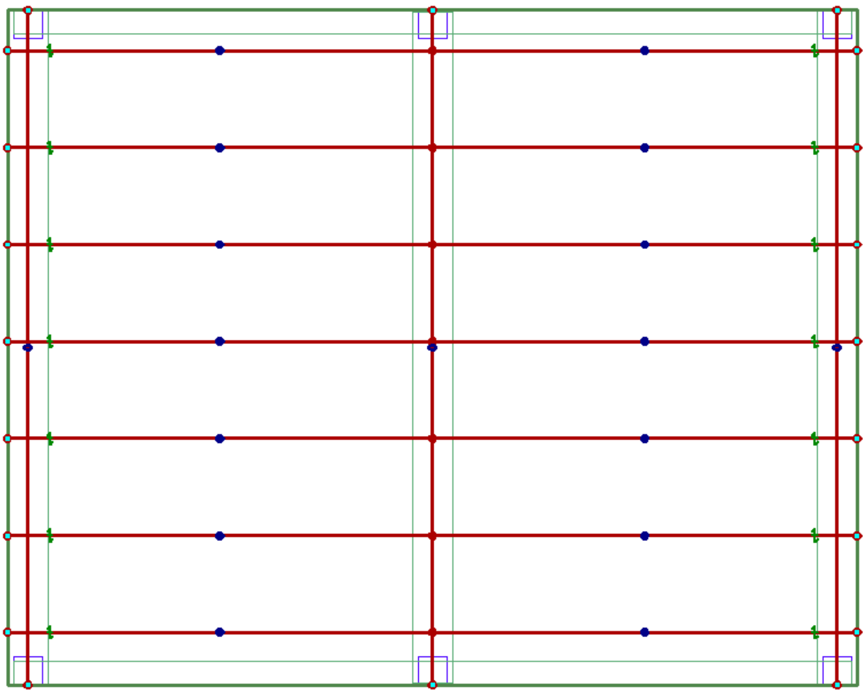

Figure 20. Layout of tendons in beams

The values of deflections at longer span (Dlt) and shorter span (Dst) of the beams were obtained from the analysis for both cases and are illustrated in Figures 21 and 22, respectively.

These deflections were compared with the maximum allowable deflection for the beams, span/250, as per the standard [27]. The maximum allowable deflection of the shorter span was 20 mm, and for the longer span, it was 32 mm. In Case (i), both the shorter and longer spans' deflections exceeded the allowable deflection limit at 600°C, whereas in Case (ii), both the shorter and longer span' deflections exceeded the allowable deflection limit at 400°C. The deflections of the longer and shorter spans in Case (i) were 57% and 12% larger than the allowable limits, respectively. In Case (ii), the deflections of the longer and shorter spans were 17% larger than the allowable limits. It is concluded that the modulus of elasticity had a significant impact on the structural performance of concrete.

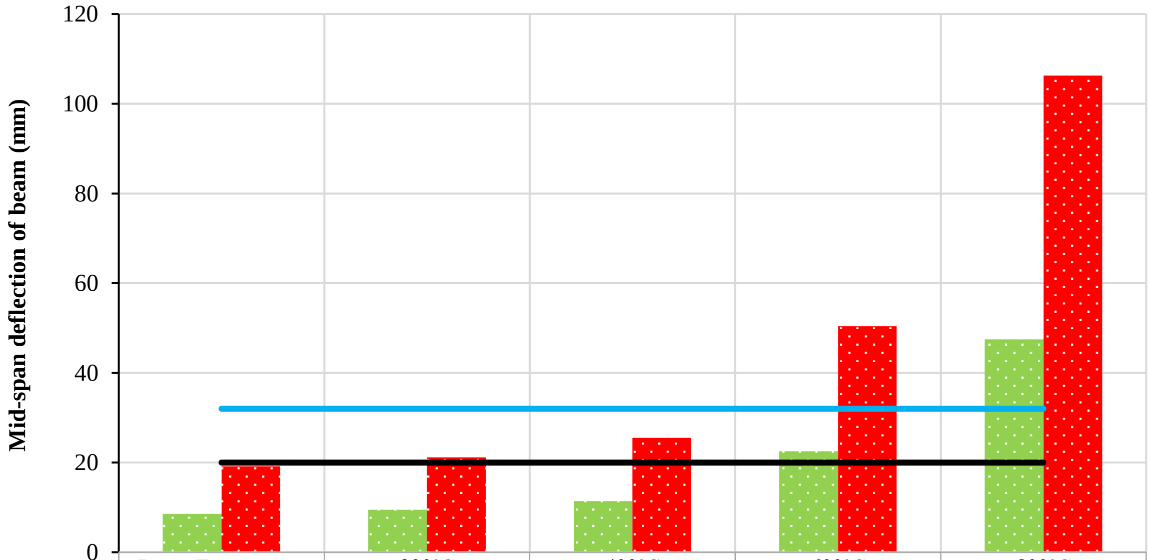

	Room Temperature	200°C	400°C	600°C	800°C
Dst	8.54	9.45	11.37	22.48	47.44
Dlt	19.13	21.18	25.49	50.35	106.28
Dst limit	20	20	20	20	20
Dlt limit	32	32	32	32	32

Figure 21. Mid-span deflections of beams for Case (i)

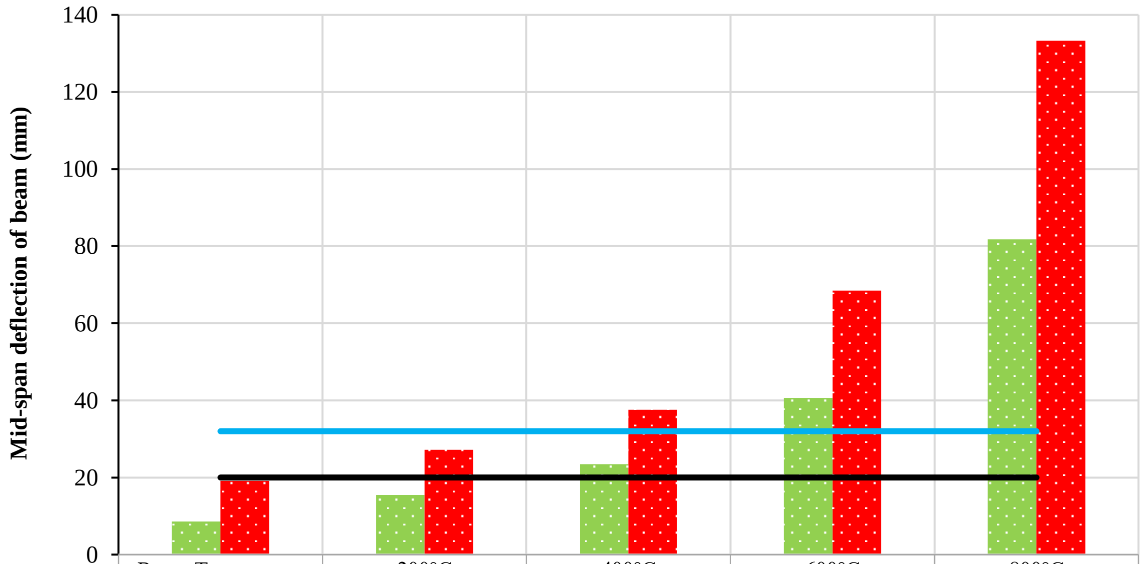

	Room Temperature	200°C	400°C	600°C	800°C
Dst	8.54	15.5	23.47	40.62	81.75
Dlt	19.13	27.23	37.58	68.49	133.29
Dst limit	20	20	20	20	20
Dlt limit	32	32	32	32	32

Figure 22. Mid-span deflections of beams for Case (ii)

4. Conclusions

The effects of elevated temperatures on M30-grade concrete were studied using various tests. Numerous specimens were cast as cubes, cylinders, and flexural beams to perform tests such as the compression, splitting tensile, and flexural tests. Water curing was adopted for the specimens for durations of 7 and 28 days. The compressive strength, splitting tensile strength, flexural strength, and modulus of elasticity were investigated. The following conclusions can be drawn from the results:

- The reduction in the moisture content present in concrete directly influenced the strength characteristics. Non-destructive tests demonstrated that concrete was deficient after 400°C.
- The geometric shapes and volume of concrete had a greater impact under high-temperature conditions.
- The strength characteristics, namely, the flexural strength, compressive strength, and tensile strength, demonstrated a drop after 400°C. This noticeably proved that concrete failed internally after 400°C.
- The microstructural studies were also evident for the concrete's internal failures due to the chemical composition changes in the specimens when they were exposed to high temperatures. The mechanical and microstructural studies were in good agreement.
- The modulus of elasticity had a considerable impact on the structural performance of the elements, and postfire structural elements became more critical.

Identifying the critical parameters of concrete under the elevated temperatures could help understand the behavior of concrete under fire. The ability to successfully design a structure to survive global collapse brought on by fire occurrences is made possible by knowledge of the material and structural behaviors. Small fire incidents in buildings may impair the essential structural performance, which eventually affects the buildings' usability and longevity. A small intensity of fire could significantly alter the post-fire performance of structures. Further full-range testing on structural elements under post-fire conditions should be carried out, as they were considered to be very critical.

5. Declarations

5.1. Author Contributions

Conceptualization, A.B. and K.S.S.; methodology, A.B. and K.S.S.; validation, A.B., K.S.S., and P.M.; formal analysis, A.B. and J.S.A.; investigation, V.M., A.B., R.S., and J.S.A.; resources, V.M. and A.B.; writing—original draft preparation, V.M., A.B. and K.S.S.; writing—review and editing, A.B. All authors have read and agreed to the published version of the manuscript.

5.2. Data Availability Statement

The data presented in this study are available on request from the corresponding authors.

5.3. Funding

The authors received no financial support for the research, authorship, and/or publication of this article.

5.4. Conflicts of Interest

The authors declare no conflict of interest.

6. References

[1] Vishal, M., & Satyanarayanan, K. S. (2022). Analytical investigation on progressive collapse of 3-D reinforced concrete frames under high temperature. Resilient Infrastructure. Lecture Notes in Civil Engineering, 202. Springer, Singapore. doi:10.1007/978-981-16-6978-1_21.

[2] Vishal, M., & Satyanarayanan, K. S. (2021). A review on research of fire-induced progressive collapse on structures. Journal of Structural Fire Engineering, 12(3), 410–425. doi:10.1108/JSFE-07-2020-0023.

[3] Khoury, G. A. (2000). Effect of fire on concrete and concrete structures. Progress in Structural Engineering and Materials, 2(4), 429–447. doi:10.1002/pse.51.

[4] Li, L. Y., Purkiss, J. A., & Tenchev, R. T. (2002). An engineering model for coupled heat and mass transfer analysis in heated concrete. Proceedings of the Institution of Mechanical Engineers, Part C: Journal of Mechanical Engineering Science, 216(2), 213–224. doi:10.1243/0954406021525142.

[5] Vishal, M., & Satyanarayanan, K. S. (2023). Study on optimum concrete cover thickness in RC beam and columns under high temperature. Journal of Structural Fire Engineering. doi:10.1108/JSFE-11-2022-0035.

[6] Murugan, V., & Srinivasan, S. K. (2022). Influence of cover thickness in structural frames exposed to fire and service loads. Environmental Science and Pollution Research, 29(57), 85955–85968. doi:10.1007/s11356-021-15925-9.

[7] Bažant, Z. P., & Prat, P. C. (1988). Effect of temperature and humidity on fracture energy. ACI Materials Journal, 85(4), 262–271. doi:10.14359/2127.

[8] Thelandersson, S. (1987). Modeling of combined thermal and mechanical action in concrete. Journal of Engineering Mechanics, 113(6), 893–906. doi:10.1061/(asce)0733-9399(1987)113:6(893).

[9] Schneider, U. (1988). Concrete at high temperatures - A general review. Fire Safety Journal, 13(1), 55–68. doi:10.1016/0379-7112(88)90033-1.

[10] Chan, S. Y. N., Peng, G. F., & Chan, J. K. W. (1996). Comparison between high strength concrete and normal strength concrete subjected to high temperature. Materials and Structures/Materiaux et Constructions, 29(10), 616–619. doi:10.1007/bf02485969.

[11] Short, N. R., Purkiss, J. A., & Guise, S. E. (2001). Assessment of fire damaged concrete using colour image analysis. Construction and Building Materials, 15(1), 9–15. doi:10.1016/S0950-0618(00)00065-9.

[12] Lee, J., & Fenves, G. L. (1998). Plastic-damage model for cyclic loading of concrete structures. Journal of Engineering Mechanics, 124(8), 892–900. doi:10.1061/(asce)0733-9399(1998)124:8(892).

[13] Schrefler, B. A., Majorana, C. E., Khoury, G. A., & Gawin, D. (2002). Thermo-hydro-mechanical modelling of high performance concrete at high temperatures. Engineering Computations, 19(7), 787–819. doi:10.1108/02644400210444320.

[14] Xu, P., Cui, Y., Dai, J., Zhang, M., & Ding, Y. (2022). High-temperature deterioration mechanism of textile-reinforced concrete with different cementitious materials. Journal of Materials in Civil Engineering, 34(1), 1–13. doi:10.1061/(asce)mt.1943-5533.0004027.

[15] Varghese, A., N, A., Arulraj G, P., & Johnson Alengaram, U. (2019). Influence of fibers on bond strength of concrete exposed to elevated temperature. Journal of Adhesion Science and Technology, 33(14), 1521–1543. doi:10.1080/01694243.2019.1602889.

[16] Zhao, J., Chen, L., Liu, G., & Meng, X. (2022). Compressive properties and microstructure of polymer-concrete under dry heat environment at 80 °C. Arabian Journal for Science and Engineering, 47(10), 12349–12364. doi:10.1007/s13369-021-06405-w.

[17] Abolhasani, A., Shakouri, M., Dehestani, M., Samali, B., & Banihashemi, S. (2022). A comprehensive evaluation of fracture toughness, fracture energy, flexural strength and microstructure of calcium aluminate cement concrete exposed to high temperatures. Engineering Fracture Mechanics, 261, 108221. doi:10.1016/j.engfracmech.2021.108221.

[18] Phan, L. T., & Carino, N. J. (1998). Review of mechanical properties of HSC at elevated temperature. Journal of Materials in Civil Engineering, 10(1), 58–65. doi:10.1061/(asce)0899-1561(1998)10:1(58).

[19] Handoo, S. K., Agarwal, S., & Agarwal, S. K. (2002). Physicochemical, mineralogical, and morphological characteristics of concrete exposed to elevated temperatures. Cement and Concrete Research, 32(7), 1009–1018. doi:10.1016/S0008-8846(01)00736-0.

[20] Nechnech, W., Meftah, F., & Reynouard, J. M. (2002). An elasto-plastic damage model for plain concrete subjected to high temperatures. Engineering Structures, 24(5), 597–611. doi:10.1016/S0141-0296(01)00125-0.

[21] Shin, K. Y., Kim, S. B., Kim, J. H., Chung, M., & Jung, P. S. (2002). Thermo-physical properties and transient heat transfer of concrete at elevated temperatures. Nuclear Engineering and Design, 212(1–3), 233–241. doi:10.1016/S0029-5493(01)00487-3.

[22] Willam, K., Rhee, I., & Shing, B. (2004). Interface damage model for thermomechanical degradation of heterogeneous materials. Computer Methods in Applied Mechanics and Engineering, 193(30–32), 3327–3350. doi:10.1016/j.cma.2003.09.020.

[23] Youssef, M. A., & Moftah, M. (2007). General stress-strain relationship for concrete at elevated temperatures. Engineering Structures, 29(10), 2618–2634. doi:10.1016/j.engstruct.2007.01.002.

[24] Caetano, H., Rodrigues, J. P. C., & Pimienta, P. (2019). Flexural strength at high temperatures of a high strength steel and polypropylene fibre concrete. Construction and Building Materials, 227, 116721. doi:10.1016/j.conbuildmat.2019.116721.

[25] Reddy, D. H., & Ramaswamy, A. (2017). Influence of mineral admixtures and aggregates on properties of different concretes under high temperature conditions I: Experimental study. Journal of Building Engineering, 14, 103–114. doi:10.1016/j.jobe.2017.09.013.

[26] IS 10262. (2019). Concrete Mix Proportioning-Guidelines. Bureau of Indian Standards, New Delhi, India.

[27] IS 456. (2000). Plain and Reinforced Concrete. Bureau of Indian Standards, New Delhi, India.

[28] Poon, C. S., Azhar, S., Anson, M., & Wong, Y. L. (2001). Comparison of the strength and durability performance of normal- and high-strength pozzolanic concretes at elevated temperatures. Cement and Concrete Research, 31(9), 1291–1300. doi:10.1016/S0008-8846(01)00580-4.

[29] Peng, G. F., & Huang, Z. S. (2008). Change in microstructure of hardened cement paste subjected to elevated temperatures. Construction and Building Materials, 22(4), 593–599. doi:10.1016/j.conbuildmat.2006.11.002.

[30] Rithin, R. K., Crasta, V., & Praveen, B. M. (2015). Enhancement of optical, mechanical and micro structural properties in nanocomposite films of PVA doped with WO_3 nanoparticles. International Journal of Structural Integrity, 6(3), 338–354. doi:10.1108/IJSI-08-2014-0036.

[31] Raja Rajeshwari, B., & Sivakumar, M. V. N. (2022). Fracture properties of fibrous self-compacting concrete using three-point bend test and wedge splitting test methods. International Journal of Structural Integrity, 13(2), 278–296. doi:10.1108/IJSI-08-2021-0093.